Article

Not peer-reviewed version

Enhanced Ocular Drug Delivery of Dexamethasone Using Chitosan-Coated Soluplus® Based Mixed Micellar System

Samer Adwan *, Faisal Al-Akayleh, Madeha Qasmieh, Teiba Obeidi

Posted Date: 25 September 2024

doi: 10.20944/preprints202409.1939.v1

Keywords: Soluplus®; Pluronic F-127; Dexamethasone; Mixed micelle; Chitosan coat

Article

Enhanced Ocular Drug Delivery of Dexamethasone Using Chitosan-Coated Soluplus® Based Mixed Micellar System

Samer Adwan [1,*], Faisal Al-Akayleh, [2] Madeiha Qasmieh, [1] and Teiba Obeidi [1]

[1] Department of Pharmaceutics and Pharmaceutical Technology, Faculty of Pharmacy, Zarqa University, Zarqa, Jordan
[2] Department of Pharmaceutics and Pharmaceutical technology, Faculty of Pharmacy and Medical Sciences, Petra University, Amman, Jordan
* Correspondence: sadwan@zu.edu.jo

Abstract: Background: This study introduces a novel dexamethasone (DEX) mixed micellar system (DEX-MM) using Soluplus® and Pluronic F-127 (PF127) to enhance ocular drug delivery. The enhancement of ocular application properties was achieved by creating a chitosan-coated DEX-MM (DEX-CMM), which promotes better adherence to the ocular surface, thereby improving drug absorption; Methods: Using the solvent evaporation method, a formulation was developed with a Soluplus® to drug ratio of 1:10, enhanced with 0.25% PF127. After dispersing in water, 1% chitosan (CS) was added. The stability and integrity of DEX within the micelles were verified using attenuated total reflection-fourier transform infrared spectroscopy (ATR-FTIR) and differential scanning calorimetry (DSC). Additionally, in vitro and ex vivo drug release studies were conducted; Results: DEX-CMM (F6) demonstrated a particle size of 151.9±1 nm and a polydispersity index (PDI) of 0.168±0.003, suggesting uniformity and high electrostatic stability with a zeta potential of +35.96±2.13 mV. The non-Fickian drug release mechanism indicated prolonged drug retention. Comparative analyses showed DEX-CMM outperforming a standard DEX suspension in drug release and ocular tissue permeation, with flux measurements significantly higher than the DEX suspension; Conclusion: The study confirmed the efficacy of DEX-CMM in enhancing drug delivery to ocular tissues, evidenced by improved permeability. Safety evaluations using the HET-CAM test demonstrated that DEX-CMM was non-irritant, supporting its potential for effective ocular drug delivery.

Keywords: Soluplus®; Pluronic F-127; dexamethasone; mixed micelle; chitosan coat

1. Introduction

The field of ocular drug delivery remains a pivotal focus in pharmaceutical research due to the intricate challenges associated with effectively treating eye-related conditions while maximizing therapeutic outcomes [1,2]. The eye's complex anatomy and physiology, characterized by barriers such as the corneal epithelium, tear film, and blood-retinal barrier, pose significant obstacles to drug delivery. These barriers often result in suboptimal drug bioavailability and therapeutic efficacy, necessitating the development of advanced delivery systems capable of navigating these challenges [3–5].

Among the therapeutic agents used in ocular treatments, DEX holds a prominent position due to its potent anti-inflammatory and immunosuppressive properties [6,7]. DEX is extensively utilized in managing ocular inflammatory conditions, particularly in diseases affecting the posterior segment of the eye, such as diabetic macular edema (DME) and posterior uveitis [8]. These conditions are associated with severe inflammation that can lead to substantial and potentially irreversible visual impairment if not adequately managed [9]. Despite its clinical efficacy, the therapeutic application of DEX is severely hampered by its physicochemical limitations, including poor water solubility, with a solubility of approximately 10 mg/L at 25°C, and a relatively short plasma half-life ranging from 3.6 to 5.5 hours [10,11]. These properties result in a need for frequent administration to maintain

 doi:10.20944/preprints202409.1939.v

therapeutic drug levels, which can be burdensome for patients and increase the risk of adverse effects [12].

Addressing these challenges requires innovative drug delivery systems that can enhance the solubility, stability, and sustained release of DEX in ocular applications [13–15]. The emergence of nanotechnology-based delivery platforms, particularly micellar systems, offers promising solutions to these limitations [16,17]. Micellar systems, formed by self-assembly of amphiphilic molecules in aqueous environments, have demonstrated significant potential in enhancing the solubility of poorly water-soluble drugs by encapsulating them within their hydrophobic core [18,19]. This encapsulation not only improves drug solubility but also stabilizes the drug, protecting it from degradation and facilitating its sustained release over time [20]. Moreover, the nanoscale size of these micelles enables them to penetrate the ocular barriers more effectively, ensuring targeted drug delivery to the affected tissues and reducing the frequency of administration required to achieve therapeutic effects [21].

In this context, the development of a DEX-MM system represents a significant advancement in ocular drug delivery [17]. This study leverages the synergistic properties of two polymers, Soluplus® and PF127, to create a robust micellar delivery system tailored for DEX. Soluplus®, a graft copolymer composed of polyethylene glycol (PEG), polyvinyl caprolactam (PVCL), and polyvinyl acetate (PVAc), is known for its amphiphilic nature, which allows it to form micelles that can effectively encapsulate hydrophobic drugs like DEX [22]. The hydrophilic shell of Soluplus® micelles ensures stability in aqueous environments, while the hydrophobic core provides a protective environment for the encapsulated drug, thereby enhancing its solubility and bioavailability [23]. Complementing Soluplus®, PF127 is a nonionic triblock copolymer that further enhances the micellar system's functionality. PF127's amphiphilic structure enables the formation of stable micelles that encapsulate hydrophobic drugs, enhancing their solubility and stability in ocular environments [24].

To further augment the therapeutic potential of the DEX-MM system, this study incorporates CS, a natural polysaccharide derived from chitin, into the formulation [25]. CS is renowned for its mucoadhesive properties, which significantly enhance the retention time of drug formulations at the site of application [26]. By prolonging contact with ocular tissues, CS facilitates sustained drug release and improves the overall bioavailability of DEX within the eye [27]. Additionally, CS enhances the permeability of drugs across the corneal epithelium, a critical barrier to ocular drug absorption, thus further improving the therapeutic efficacy of the delivery system [28]. The biocompatibility and biodegradability of CS also align with the safety requirements for ocular formulations, making it an ideal component for advanced drug delivery systems [29].

The novelty of this research lies in the strategic combination of Soluplus®, PF127, and CS to develop a mixed micellar delivery system that addresses the critical therapeutic needs in ocular drug delivery. By optimizing drug encapsulation efficiency, enhancing solubility, and promoting a sustained release profile, this innovative approach offers a potential breakthrough in the treatment of ocular diseases. This system not only aims to improve the bioavailability of DEX but also seeks to reduce the frequency of administration and minimize the risk of side effects, thereby improving patient compliance and quality of life. The findings of this research have the potential to improve clinical outcomes for patients suffering from severe ocular diseases, ultimately contributing to better quality of life and reduced healthcare costs associated with these conditions.

2. Materials and Methods

2.1. Material

Low molecular weight chitosan (STBH6262), and Pluronic F-127 (BCCB3537) were purchased from Sigma-Aldrich® (Missouri, USA). Dexamethasone (AB115220) was purchased from ABCR GmbH (Karlsruhe, Germany). Soluplus® (402932-23-4) was a gift from BASF Pharma (New Jersey, USA). Glacial acetic acid and ethanol was purchased from Honeywell®, (Raunheim, Germany). Acetonitrile HPLC grade was purchased from Sisco Research Laboratories Pvt Ltd (Mumbai, India).

2.2. Methods

2.2.1. Preparation of DEX-MM and DEX-CMM

 doi:10.20944/preprints202409.1939.v

The preparation of DEX-MM involved the solvent evaporation method to encapsulate DEX within mixed micelles composed of Soluplus® and P F127. Soluplus®, PF127, and DEX were dissolved in ethanol, utilizing the minimal amount required for complete dissolution of polymers and drug. A 0.1% concentration of DEX, representative of the topical dose in ophthalmic formulations, was loaded at different ratios of Soluplus® to PF127. Three distinct ratios of Soluplus® to PF127 were utilized to explore their impact on the properties of the micellar systems. Specifically, the ratios of Soluplus® to PF127 employed were 1:1, 2:1, and 4:1, respectively. This solution was then subjected to vacuum drying (BINDER GmbH, Tuttlingen, Germany) at -0.1 MPa and 45°C to remove the ethanol, resulting in a transparent polymeric film representing a solid dispersion (SD). This SD was subsequently rehydrated in 10 mL of either phosphate-buffered saline (PBS), adjusted to a pH of 7.4, or deionized water, with stirring continued overnight at 100 rpm to ensure thorough dispersion.

Low molecular weight CS was employed for the coating process. CS was initially dissolved in a 1% w/v acetic acid solution to facilitate solubility. The concentrations of CS added varied between 0.25, 0.5, 1 and 2 mg/ml. This prepared solution was subsequently added dropwise to the micellar dispersion, ensuring a uniform coating of the micelles. Following the addition, the mixture was stirred overnight at 25°C and 100 rpm to facilitate stable coating formation on the micelles. The final micellar formulation was filtered through a 0.22 µm membrane to ensure sterility and uniformity (Figure 1). The formulation selection was based on achieving the optimal particle size and ensuring stability of the dispersion during storage, both of which are critical factors for effective ocular drug delivery. The composition of the selected formulations is detailed in Table 1. The content of DEX was determined by HPLC assay after diluting the micelles with acetonitrile.

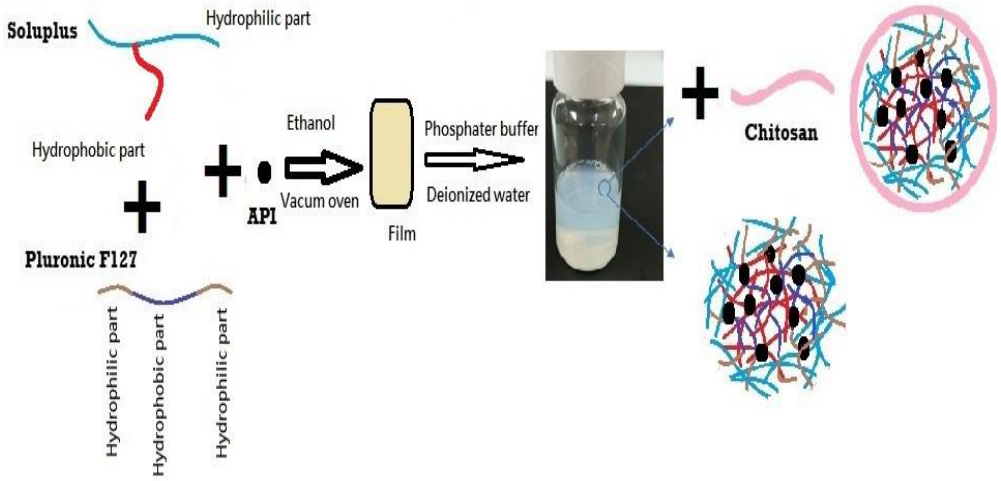

Figure 1. Schematic representation of the formulation process for DEX-MM and DEX-CMM.

Table 1. Composition of selected formulations. Concentrations expressed in mg/ml.

Formulation	Soluplus®	PF127	CS	DEX	Medium
F1	10	25	0	1	PBS
F2	10	25	0.5	1	PBS
F3	10	25	1	1	PBS
F4	10	25	0	1	DDW
F5	10	25	0.5	1	DDW
F6	10	25	1	1	DDW

2.2.2. Characterization of DEX-MM and DEX-CMM

 doi:10.20944/preprints202409.1939.v

The particle size, PDI, and zeta potential of DEX-MM and DEX-CMM were measured by dynamic light scattering using a Malvern system (Malvern ZE S.A., Worcestershire, UK).

2.2.3. Analytical Method

JASCO LC-4000 Series HPLC system (Japan), with a binary pump, degasser, autosampler, and UV detector, was used for DEX analysis. Samples were analyzed by reversed-phase chromatography. A column from Fortis® ODS-C18 (250 x 4.6 mm ID, 4 μm) RP-18 was used. The flow rate was 0.8 ml/min, and the UV detection was 245 nm. Autosampler temperature was maintained at a temperature of 25°C. The autosampler temperature was maintained at a temperature of 25°C. The mobile phase consisted of 60% deionized HPLC-grade water and 40% acetonitrile. The mobile phase was degassed using sonication for 60 min. The column was conditioned with the mobile phase for at least 90 min each time before use. Samples (20 μL) were injected into the HPLC system. The DEX calibration curve was made by preparing solutions containing increasing amounts of DEX (range 1-100 μg/ml) and plotting their respective UV absorption against their respective drug concentrations.

2.2.4. Calculation of the Encapsulation Efficiency (%EE)

The prepared DEX-MM and DEX-CMM were isolated from the unloaded DEX using an indirect method by dialysis membrane. Samples were withdrawn from the dialysis medium and then analyzed using HPLC to calculate %EE. The encapsulation efficiency was calculated by first subtracting the free DEX amount from the total DEX amount. The resulting value was then divided by the total DEX amount, and the quotient was multiplied by 100% to obtain the %EE.

2.2.5. ATR-FTIR Studies

ATR-FTIR (PerkinElmer®, Llantrisant, UK) was employed to analyze the physical/chemical interaction between pure components and engineered formulations. In this study, determination of possible interaction of DEX with formulation components. Individual components as polymers, drug, their physical mixture and the SD was examined by ATR-FTIR spectrometer. Physical mixtures were prepared by intimate trituration of equimolar quantities 20 mg of individual components in an agitation by mortar for 10 min to obtain a homogenous mixture. Samples were placed directly on the small crystal spot after cleaning with methanol and then the arm was reversed and rotated down to push the sample down onto the crystal phase for better contact.

2.2.6. DSC Studies

Thermal analysis of DEX and SD was performed using DSC 4000 differential scanning calorimeter (Perkin-Elmer, Waltham, MA, USA). Five milligrams of samples were used for DSC. Temperature scans were performed in the temperature range 25–350°C at a heating rate of 25°C /min, under a nitrogen purge gas flow of 20 mL/min.

2.2.7. In Vitro Release Study

The in vitro release behaviour of DEX from the micellar formulations DEX-MM (F4) and DEX-CMM (F6) was assessed using the dialysis bag diffusion method. For comparative analysis, a free DEX suspension served as the control. Each sample consisted of 1 mL of the respective formulation, with a concentration of 1 mg/mL of DEX, was enclosed in a dialysis membrane bag with a molecular weight cut-off of 12,000 g/mol (Green Bird Inc., Shanghai, China). These bags were then submerged in 50 mL of PBS and maintained at 37°C to simulate physiological conditions. The completely released DEX was under the sink condition. At predetermined time intervals, triplicate aliquots of the release medium were withdrawn for analysis and immediately replenished with fresh PBS to keep the volume constant. The concentration of DEX released into the supernatant was quantitatively determined using HPLC.

2.2.8. Ex Vivo Permeation Study

 doi:10.20944/preprints202409.1939.v

Sheep eyes were obtained from a local slaughterhouse, and the eyeballs were immediately collected after the sheeps were sacrificed. The eyeballs were transported in a cold PBS solution. Only the eyeballs that were transparent and had undamaged cornea were selected. Then, the corneal tissues were removed with scalpels and scissors, washed with PBS, and stored in normal saline at 4°C until permeation study. An ex vivo permeation study using corneal tissue was performed with Franz-diffusion cells having an effective diffusion area of 0.672 cm^2. The receptor chamber, with a capacity of 5 mL, was filled with PBS adjusted to a pH of 7.4, and the receptor medium was stirred at 600 rpm. Corneal tissues were carefully placed on a Franz-diffusion cell, and 300 µL of F4 and F6 was applied to the donor chamber. All formulations contained 0.1 w/v % of DEX. Franz diffusion cell was maintained at 37°C with a thermostat. A 0.5-mL sample was taken every hour from the receptor chamber for 5 h and immediately replenished with an equal volume of PBS. The permeability of the drug in each formulation was evaluated by plotting the cumulative permeated amount of DEX per unit area (µg/cm^2) over time (h). The steady-state flux (Js) across the porcine corneal tissue was calculated from the slope of the linear portion of the cumulative permeation graph. All samples were diluted appropriately and analyzed by HPLC. Each experiment was repeated in triplicate.

2.2.9. Morphology Observation by Transmission Electron Microscope (TEM)

Transmission electron microscopy (TEM) imaging was performed to characterize polymeric micelles using an H-7600 transmission electron microscope (Hitachi, Tokyo, Japan), with an accelerating voltage of 100 kV. The samples were stained with 2% phosphotungstic acid, placed on a copper grid, and exposed under an infrared lamp for 10 min.

2.2.10. Physical Stability Test

In order to evaluate the physical stability of mix micelles, the DEX-CMM (n=3) were stored at 4°C for 15 days, then the average size, PDI and clarity of the micelles system were monitored. Moreover, Robustness of DEX-CMM for dilution was assessed by exposing them to 50 and100-fold dilution with water and PBS. The diluted formulations were stored for 24 h and monitored for any physical changes (such as precipitation or phase separation).

2.2.11. In Vitro Ocular Irritation Testing Using the Hen's Egg Test-Chorioallantoic Membrane (HET-CAM)

Fresh and fertilized hens' eggs were incubated at 37°C for 10 days. The eggs were rotated three times daily to avoid sticking the embryo on one side of the egg. After 10 days, the eggs were candled to mark the air space and to discard defective eggs. The eggshell around the air space was removed using blade and scissors. The inner membrane was detached using forceps to reveal the chorioallantoic membrane (CAM). F6 and controls (0.2 mL) were applied over the CAM for 5 min. NaCl solution 0.9% w/v and NaOH solution 10% w/v were applied as controls. The test was performed in triplicate. Possible hemorrhage, vascular lysis or coagulation of CAM vessels were recorded for 5 min. Then, the irritation score (IS) was calculated according to a previously reported method [30].

2.2.13. Statistical Analysis

Statistical analysis of the experimental results was conducted using either t-test analysis or one-way analysis of variance (ANOVA), depending on the experimental design and the data distribution. These analyses were performed using GraphPad Prism software (version 6; GraphPad, Inc., San Diego, CA, USA). For the purposes of this study, a p-value less than 0.05 was considered to indicate a statistically significant difference between the tested groups.

3. Results and Discussion

3.1. Preparation and Physicochemical Characterization

In this study, a novel formulation was developed by coating a mixed micellar system of Soluplus® and PF127 with CS to achieve improved stability and ocular drug permeation of DEX.

 doi:10.20944/preprints202409.1939.v

Soluplus® exhibits an exceptionally low critical micelle concentration (CMC) and forms highly stable micelles against dilution [23]. In our study, the concentration of Soluplus® employed exceeded the CMC (6.6 x 10^{-5}), ensuring a stable dispersion. A 0.1% concentration of DEX, representative of the topical dose in ophthalmic formulations, was loaded at different ratios of Soluplus® to PF127. Ethanol was utilized as a solvent for the formulation because it offers excellent solubility for both hydrophilic and hydrophobic components such as DEX, Soluplus®, and Poloxamer F127 [31]. Moreover, Ethanol's advantageous properties include low toxicity and high volatility, which facilitate its complete removal by vacuum drying at controlled temperatures, preserving the stability and integrity of the active ingredients and polymers [32]. A mixture of 100 and 2.5 mg/ml of Soluplus® to PF127 resulted in a stable dispersion with optimum size for ocular drug delivery. Zhang *et al*. (2017) elucidated the efficacy of a Soluplus®/PF127 mixed micellar system in augmenting the oral bioavailability of apigenin. This innovative system significantly enhanced the solubility and oral bioavailability of apigenin, underscoring the considerable potential of mixed micelles for advanced drug delivery. Leveraging a core-shell architecture, the system markedly improves the stability and solubility of hydrophobic drugs, facilitating superior absorption at targeted sites [33].

The addition of CS solution to nanoparticle dispersions is an efficient and straightforward method for CS coating, highly advantageous in pharmaceutical applications due to its ability to enhance colloidal stability, increase bioadhesion, and control drug release [34]. CS concentrations ranging from 0.02 mg/mL to 10 mg/mL have been reported for coating various nanoparticles, with different effects on size, zeta potential, and coating efficiency [35]. In this study, two concentrations of CS, specifically 0.5 and 1 mg/mL, successfully produced a stable dispersion with an optimum particle size. The data presented in Table 2 indicates that the particle size and PDI of the selected formulations are within the optimal range for ocular drug delivery. For effective penetration through ocular barriers and to minimize irritation to the eye, nanosystems intended for this purpose should have a particle size between 10 to 200 nanometers [36]. Moreover, an ideal PDI, typically less than 0.3, is crucial as it indicates a uniform size distribution of the particles. This uniformity is essential for maintaining consistent pharmacokinetic profiles, ensuring efficient penetration through the ocular barriers, and avoiding mechanical irritation to the sensitive tissues of the eye [37]. The dispersion medium and CS concentration were primary factors influencing the particle size and zeta potential of the micelles. The size of the micelles decreased in PBS compared to those dispersed in water due to micelle contraction owing to the higher ionic strength of the medium. CS` addition resulted in a notable increase in particle size, particularly when dispersed in water, attributed to electrostatic attraction between the electronegative oxygen atoms in Soluplus® and PF127 and the electropositive CS chain, as well as hydrogen bonding between oxygen atoms of Soluplus® and PF127 and hydroxyl groups of CS.

Table 2. Characterization of DEX-MM and DEX-CMM formulations, (Mean±SD, n=3).

Code	Size (nm)	PDI	Zeta potential (mV)	%EE
F1	76.9±0.8	0.160±0.004	-3.17±0.74	81.32±1.96
F2	92.2±0.2	0.139±0.007	- 0.59±1.34	75.62±2.93
F3	107±0.1	0.125±0.007	3.20±1.87	76.90±1.02
F4	69.1±0.6	0.053±0.007	-4.37±0.57	89.44±1.37
F5	118.5±1.5	0.157±0.004	0.26±0.36	85.50±1.90
F6	151.9±1	0.168±0.003	35.96±2.13	91.95±0.46

The addition of CS shifted the zeta potential toward more positive values, with a greater effect observed in water than in PBS. The zeta potential of DEX-MM was shifted from -3.17±0.74 to -0.59±1.34 and 3.20±1.87 by the addition of 0.5 mg/mL and 1 mg/mL CS, respectively, and dispersion in PBS. While the charge was shifted from -4.37±0.57 to 0.26±0.36 and 35.96±2.13 by the addition of 0.5 mg/mL and 1 mg/mL CS, respectively, and dispersion in water. Pepic *et al*. (2008) provided

 doi:10.20944/preprints202409.1939.v

insights into how different parameters influence the properties of CS and surfactant-based nanoparticle systems. They reported that higher ionic strength in the dispersion medium can diminish electrostatic repulsions by shielding charges on CS and surfactant molecules, leading to larger particle sizes due to aggregation and a reduction in zeta potential by compressing the electrical double layer around the particles [38]. Additionally, higher concentrations of CS result in larger particle sizes due to increased viscosity and the formation of a thicker polymer layer, although excessively high concentrations may cause agglomeration. Conversely, the zeta potential increases with CS concentration, enhancing electrostatic stability and preventing aggregation [39]. At acidic pH levels, CS is more soluble, leading to smaller particles and higher zeta potential due to increased protonation, whereas at higher pH, decreased solubility and protonation of CS lead to larger particles and lower zeta potential [38]. Micelles with higher zeta potentials typically exhibit greater electrostatic repulsion between particles, resulting in improved stability against aggregation and precipitation [40]. This enhanced stability ensures prolonged circulation time in biological fluids, facilitating targeted drug delivery to specific sites in the body. Moreover, the zeta potential of Soluplus®-PF127 mixed micellar systems can influence their interaction with biological membranes and cellular uptake. Positively charged micelles, indicated by higher zeta potentials, tend to adhere more strongly to negatively charged cell surfaces, promoting cellular internalization and enhancing drug delivery efficiency [41]. This property is particularly valuable for improving the bioavailability and therapeutic efficacy of poorly water-soluble drugs by facilitating their transport across biological barriers [42].

3.2. ATR-FTIR Studies

Figure 2 illustrates the distinctive spectral features observed in the infrared spectra of pure DEX, Soluplus® and PF127. In the DEX spectrum, characteristic absorption bands were detected at 3390 cm^{-1} and 1268 cm^{-1}, attributed to the stretching vibrations of O-H and C-F bonds, respectively. Additionally, peaks at 1706 cm^{-1}, 1662 cm^{-1}, and 1621 cm^{-1} indicated the presence of C-O and double bond framework conjugated to C-O bonds [43]. The Soluplus® spectrum displayed characteristic bands at 1730 cm^{-1} (corresponding to ester carbonyl stretching) and 1632 cm^{-1} (representing tertiary amide carbonyl), consistent with previous studies [44]. Furthermore, the PF127 spectrum exhibited signals associated with the stretching vibrations of various bonds: 2880 cm^{-1} (C–H stretch), 1278 cm^{-1}, and 1240 cm^{-1} (C–O–C stretches), and 1097 cm^{-1} (C–O stretch) [45]. Upon examining the physical mixture and the SD, it was evident that while the characteristic signals of DEX and the polymers were present in the spectra of the physical mix, SD displayed a reduction in the intensity of DEX absorption peaks. This reduction suggests the occurrence of intermolecular interactions and entrapment of DEX within the SD formulation [46]. This observation underscores the potential role of intermolecular interactions in the formation and stability of DEX-loaded micelles, which could influence their physicochemical properties. These findings contribute to our understanding of the structural characteristics of the developed formulations and their potential applications in drug delivery systems.

 doi:10.20944/preprints202409.1939.v

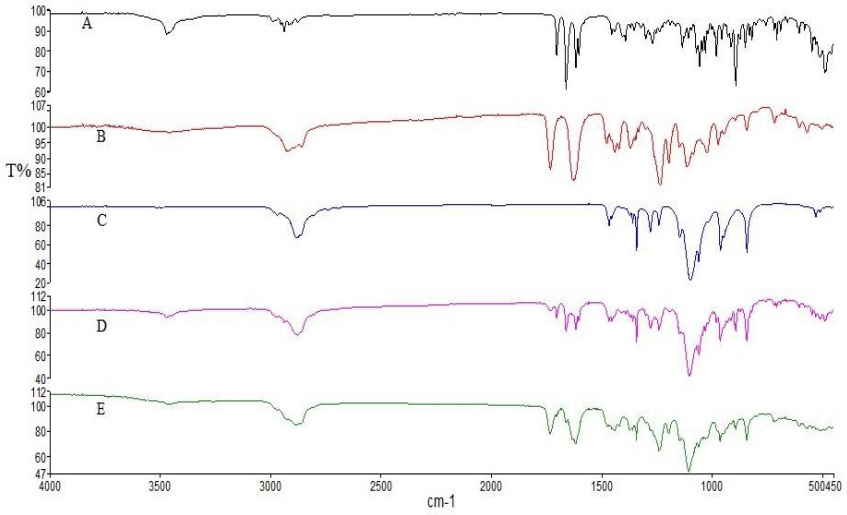

Figure 2. FTIR fingerprint of individual components, physical blend and SD: DEX (A), Soluplus® (B), PF127 (C), physical mixture (D) and (E) SD.

3.3. DSC Studies

DSC analysis provided insightful data on the thermal properties of pure DEX and its formulation (SD). As shown in Figure 3, the DSC thermogram of pure DEX displayed a distinct endothermic peak, suggesting a melting point ranging between 280-290°C. This peak is characteristic of the crystalline nature of pure DEX [47]. In contrast, the DSC thermogram of the SD showed a significant alteration; the characteristic melting peak of DEX was absent. This absence indicates a transformation in the physical state of DEX within the micelles, from crystalline to amorphous [47]. Such a transformation is indicative of the effective encapsulation of DEX within the micelle matrix, where the drug is molecularly dispersed and no longer exists in its crystalline form.

This finding is crucial as it suggests that the drug is well-integrated into the micelles, potentially enhancing its solubility and stability. Thus, the development of DEX-CMM could represent a significant advancement in the formulation of DEX for enhanced drug delivery.

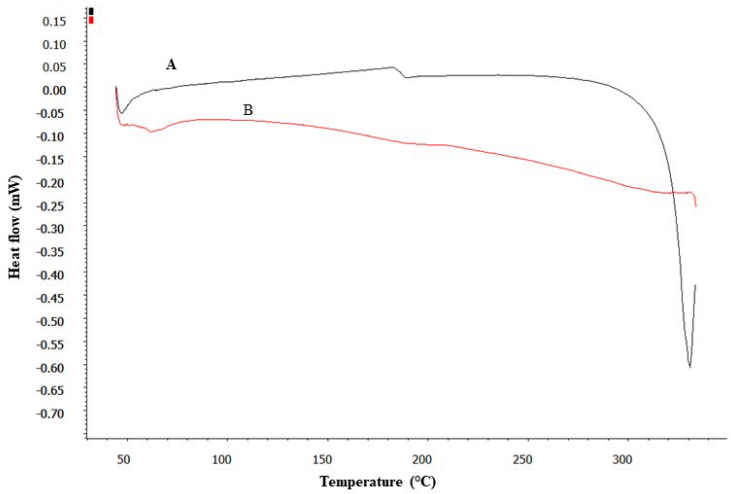

Figure 3. DSC thermograms of pure DEX (A) and the SD (B).

3.4. In Vitro Drug Release

Figure 4 illustrates the in vitro release profiles of DEX from DEX-suspension, F4 (DEX-MM) and F6 (DEX-CMM) in PBS. The results demonstrate a significant enhancement in drug release from both

 doi:10.20944/preprints202409.1939.v

DEX-MM and DEX-CMM compared to DEX-suspension ($p > 0.05$). This augmented release can be attributed to the solubilizing effect of Soluplus® and PF127 on the drug. After 1 hour, DEX exhibited a percentage release of 10.57±0.79% and 12.70±1.06% from formulations F4 and F6, respectively, while the released amounts after 7 hours were 35.53±0.83% and 40.50±0.75% from F4 and F6, respectively. Statistical analysis revealed no significant difference in release over the first 3 hours ($p > 0.05$), whereas a significant difference was observed after 3 h ($p < 0.05$) between F4 and F6. This suggests that the addition of CS to the system significantly influenced the drug release rate compared to the DEX-MM system. To determine the most appropriate kinetic model for describing the release of DEX from DEX-CMM, several models were assessed, including First-order, Zero-order, Higuchi, and Korsmeyer-Peppas. The corresponding R^2 values were 0.7592, 0.9350, 0.9624, and 0.9555, respectively, with a release exponent (n) of 0.65 for the Korsmeyer-Peppas model. Notably, the highest correlation with experimental data was observed with the Higuchi model, which presented an R^2 of 0.9624. This suggests that the release of DEX from the micelles is primarily governed by diffusion through a homogeneous matrix. Such a diffusion-controlled process is typical for systems where the drug gradually diffuses out of a polymeric network [48]. Moreover, the Korsmeyer-Peppas model, which also exhibited a high R^2 of 0.9555, provides further insight into the complexities of the release mechanism. The release exponent of 0.65 indicates anomalous (non-Fickian) diffusion, where both the diffusion of the drug and the erosion of the polymeric matrix contribute to the release process [49]. This dual mechanism is particularly pertinent to CS -coated systems, where the polymer may undergo swelling or erosion, thereby influencing the release dynamics [50]. Additionally, the CS coating modifies the release behavior by adding a physical barrier that the drug molecules must traverse, further affecting the release kinetics [51].

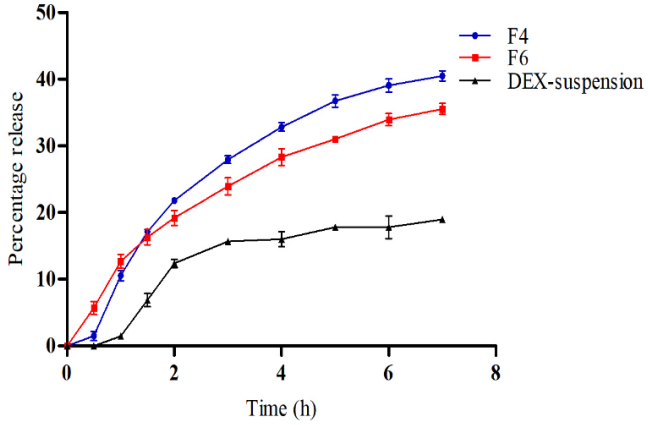

Figure 4. The in-vitro drug release results. Plotted in terms of % released of DEX vs. time for DEX-suspension, DEX-MM and DEX-CMM (Mean±SD, n=3).

3.5. Ex Vivo Drug Permeation

To evaluate the permeation and penetration capabilities of DEX, sheep corneal tissues were employed as an ex vivo model (Figure 5). The study compared three formulations: F4, F6, and a DEX-suspension. The results indicated that DEX permeated the corneal tissues from both F4 and F6 with a lag time of 1.5 hours. In contrast, the DEX-suspension exhibited a significantly delayed permeation, with drug permeation commencing only after 4 hours. The flux (Js) values were calculated to quantify the permeation rates. The DEX-suspension displayed a flux of 0.65±0.05 mg/cm²/h, which was substantially lower compared to the F4 and F6 ($p < 0.05$), which showed flux values of 4.92±0.02 mg/cm²/h and 5.63±0.13 mg/cm²/h, respectively. These findings highlight the superior permeation capabilities of the micellar formulations over the traditional suspension. The lag time of 1.5 hours for the micellar formulations suggests a rapid initial uptake of DEX through the corneal barrier, likely facilitated by the enhanced solubility and stability provided by the micelles. In contrast, the prolonged lag time for the DEX-suspension underscores the challenges of delivering hydrophobic

 doi:10.20944/preprints202409.1939.v

drugs across the corneal barrier using conventional suspension formulations. The significantly higher flux values for the micellar systems, particularly the CS -coated micelles, underscore the beneficial impact of CS in enhancing drug permeation. CS can temporarily disrupt tight junctions between corneal epithelial cells, facilitating paracellular drug transport and enhancing drug permeation across the cornea. Furthermore, CS's positive charge allows electrostatic interactions with negatively charged mucin glycoproteins present on the ocular surface, leading to increased residence time and improved drug absorption [52].

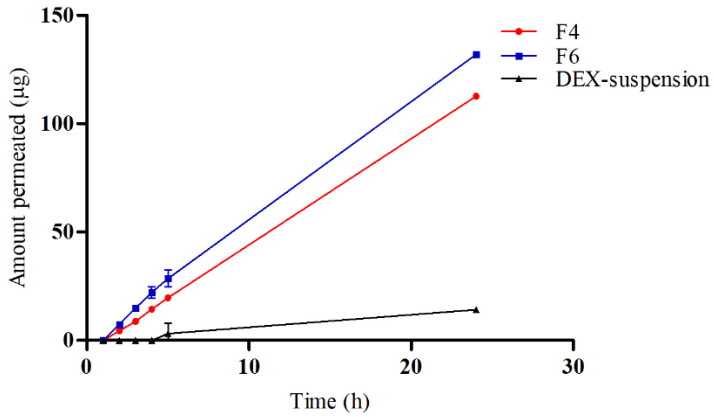

Figure 5. Ex-vivo permeation study results of DEX-suspension, DEX-MM and DEX-CMM through corneal tissue using Franz cell, (Mean±SD, n=3).

3.6. Morphology Observation by Transmission Electron Microscope (TEM)

The morphological characteristics of formulations F4 and F6, corresponding to DEX-MM and DEX-CMM respectively, were meticulously analyzed using TEM. The TEM images, displayed in Figure 6, illustrate the distinct morphologies of DEX-MM and DEX-CMM under various magnifications. Figure 5 highlights that DEX-MM and DEX-CMM micelles are predominantly round in shape and exhibit minimal aggregation. Notably, the surface-modified nanomicelles (DEX-CMM) are more compact and have a larger diameter. This is speculated to result from the micelles being coated with multiple entangled CS molecular chains, which enhances their structural integrity [53]. The CS enhancement on the surface of DEX-CMM offers improved stability and increased residence time on ocular surfaces, making them highly suitable for use as carriers in ophthalmic drug delivery systems [54].

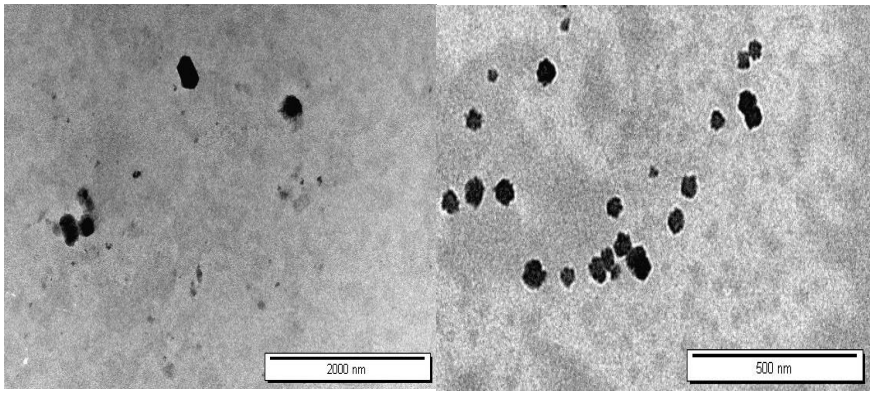

(a) (b)

Figure 6. TEM images of F6 (a) and F4 (b).

3.7. Physical Stability of DEX-CMM

 doi:10.20944/preprints202409.1939.v

The physical stability of formulations F6 was assessed after storage at 4°C. Data presented in Table 3 indicates that both the average particle size and the PDI remained stable, showing no significant changes after a 15-day storage period at this temperature. Additionally, the formulation remained clear throughout the storage period, showing no signs of aggregation or precipitation. This stability underscores the robustness of the formulation under refrigerated conditions, highlighting their potential for sustained use in clinical settings [55]. Additionally, F6 was exposed to different folds of dilution in PBS to mimic the in vivo conditions where the formulation would encounter gradual dilution. The formulation was subjected to 50 and 100-fold dilution in PBS [56]. Formulation showed no signs of precipitation, cloudiness or separation for 24 h.

Table 3. Physical stability of F6 over time at 4°C (Mean ±SD, n=3).

Time (d)	1	3	7	10	15
Size (nm)	151.9±1	148.4±1.2	151.4±1.7	149.2±0.5	145.9±3.1
PDI	0.168±0.003	0.166±0.001	0.187±0.007	0.182±0.008	0.197±0.011

3.8. In Vitro Ocular Irritation Testing Using HET-CAM

The potential irritancy of substances on the eye was studied in-vitro using the HET-CAM. Applying the HET-CAM offers many advantages, one of which the well-developed vascularization of the CAM as a tissue containing arteries, veins and capillaries which responds well to injury with an inflammatory reaction similar to that observed in the rabbits' conjunctival tissue. The second advantage is the reduced cost (due to the reduction in the number of mammals being used), time and suffering of the mammals [57,58]. As presented in Figure 7, it is apparent that the positive control (10% NaOH) was severely irritant, in contrast the negative controls (aqueous; 0.9% NaCl) produced non-irritant response. F6 was found to be practically non-irritant when applied to the surface of the CAM because none haemorrhage, vascular lyses or coagulation of CAM vessels was observed along the 5 min of the test.

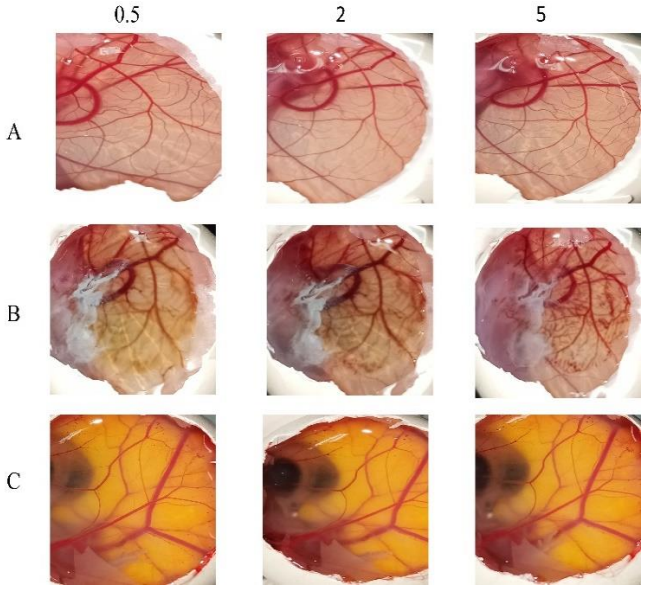

Figure 7. HET-CAM analysis depicting the response to F6 (A), 10% w/v NaOH as a positive control (B), and normal saline solution as a negative control (C). Images captured at 0.5, 2, and 5 minutes post-application illustrate the comparative irritancy and biocompatibility of the formulations.

5. Conclusions

This study heralds a significant advancement in ocular drug delivery by developing and thoroughly characterizing DEX-CMM. By incorporating Soluplus® and PF127, the micelles enhance the solubility and stability of DEX well beyond its critical micelle concentration, resulting in a stable

 doi:10.20944/preprints202409.1939.v

and efficacious dispersion suitable for ocular application. This addresses common issues with conventional DEX treatments, which often suffer from poor solubility and instability. Additionally, the integration of CS significantly boosts the mucoadhesive properties of the system, leading to extended drug retention on the ocular surface and improved permeation through the ocular barriers. This is particularly beneficial for treating diseases affecting the posterior segment of the eye, where traditional methods frequently fall short.

The study also establishes that DEX-CMM achieves an optimal particle size and zeta potential, which are crucial for maximizing bioavailability and ensuring stable, effective, and irritation-free delivery to the targeted ocular tissues. These characteristics underline the potential of DEX-CMM to enhance therapeutic outcomes significantly.

Looking forward, it is crucial to explore the long-term stability of DEX-CMM under various storage conditions to ensure its efficacy over extended periods. Additionally, in vivo studies are essential to assess the pharmacodynamics, pharmacokinetics, and long-term safety of DEX-CMM, providing deeper insights into its clinical relevance and therapeutic potential. Addressing the scalability challenges of this innovative formulation will also be vital for its successful transition from laboratory to clinical use. Further research should also expand on the bioefficacy of DEX-CMM across different ocular conditions to fully understand its therapeutic versatility and potential.

In conclusion, this research significantly contributes to pharmaceutical sciences by offering a sophisticated ocular drug delivery system that promises to enhance treatment protocols and improve patient outcomes in eye care. The results encourage ongoing exploration and optimization of micellar systems enhanced with biocompatible materials like CS, aiming to overcome the longstanding challenges of effective ocular disease management.

Author Contributions: Conceptualization, supervision, and writing of the original draft, Samer Adwan. Methodology, data curation, software, Madeiha Qasmieh. Formal analysis, provision of study resources, validation of results, Faisal Al-Akayleh. Methodology, Teiba Obeidi. All authors have read and agreed to the published version of the manuscript.

Funding: The authors gratefully acknowledge the funding and support provided by the Deanship of Scientific Research at Zarqa University, which was instrumental in conducting this research.

Institutional Review Board Statement: Not applicable.

Informed Consent Statement: Not applicable.

Data Availability Statement: The data that support the findings of this study are available from the corresponding author, (Samer Adwan).

Acknowledgments: This work was supported by the Deanship of Scientific Research at Zarqa University. We express our gratitude for their continued support and resources, which greatly facilitated the completion of this research. We also extend our heartfelt thanks to Dr. Saja Hamed from Hashemite University and Dr. Hatim Alkhatib from the University of Jordan for their invaluable assistance in the characterization of the developed micellar system.

Conflicts of Interest: The authors declare that there are no competing interests regarding the publication of this paper.

References

1. Hellinen, L., Hongisto, H., Ramsay, E., Kaarniranta, K., Vellonen, K. S., Skottman, H., & Ruponen, M. Comparison of barrier properties of outer blood-retinal barrier models–Human stem cell-based models as a novel tool for ocular drug discovery. *Eur. J. Pharm. Biopharm*. 2023, 184, 181-188. https://doi.org/10.1016/j.ejpb.2023.05.018.
2. Han, H., Li, S., Xu, M., Zhong, Y., Fan, W., Xu, J., ... & Yao, K. Polymer-and lipid-based nanocarriers for ocular drug delivery: current status and future perspectives. *Adv. Drug Deliv. Rev*. 2023, 196, 114770. https://doi.org/10.1016/j.addr.2023.114770.
3. Aragón-Navas, A., López-Cano, J. J., Johnson, M., Sigen, A., Vicario-de-la-Torre, M., Andrés-Guerrero, V., ... & Herrero-Vanrell, R. Smart biodegradable hydrogels: Drug-delivery platforms for treatment of chronic

ophthalmic diseases affecting the back of the eye. *Int. J. Pharm*. 2024, 649, 123653. https://doi.org/10.1016/j.ijpharm.2024.123653.

4. Faria, M. J., González-Méijome, J. M., Oliveira, M. E. C. R., Carracedo, G., & Lúcio, M. Recent advances and strategies for nanocarrier-mediated topical therapy and theranostic for posterior eye disease. *Adv. Drug Deliv. Rev*. 2024, 115321. https://doi.org/10.1016/j.addr.2024.115321.
5. Jain, A., Bhardwaj, K., & Bansal, M. Polymeric Micelles as Drug Delivery System: Recent Advances, Approaches, Applications and Patents. *Curr. Drug Saf*. 2024, 19 (2), 163-171. https://doi.org/10.2174/1574886319666190121095632.
6. Butt, F., & Devonport, H. Treatment of non-infectious posterior uveitis with dexamethasone intravitreal implants in a real-world setting. *Clin. Ophthalmol*. 2023, 601-611. https://doi.org/10.2147/OPTH.S123456.
7. Won, J., Kang, J., & Kang, W. Comparative Ocular Pharmacokinetics of Dexamethasone Implants in Rabbits. *J. Ocul. Pharmacol. Ther*. 2024. https://doi.org/10.1089/jop.2024.0057.
8. Gaballa, S. A., Kompella, U. B., Elgarhy, O., Alqahtani, A. M., Pierscionek, B., Alany, R. G., & Abdelkader, H. Corticosteroids in ophthalmology: Drug delivery innovations, pharmacology, clinical applications, and future perspectives. Drug Deliv. *Transl. Res.* 2021, 11, 866-893. https://doi.org/10.1007/s13346-021-00918-1.
9. Qi, Q., Wei, Y., Zhang, X., Guan, J., & Mao, S. Challenges and strategies for ocular posterior diseases therapy via non-invasive advanced drug delivery. *J. Control. Release*. 2023, 361, 191-211. https://doi.org/10.1016/j.jconrel.2023.191211.
10. Valtari, A., Posio, S., Toropainen, E., Balla, A., Puranen, J., Sadeghi, A., ... & Del Amo, E. M. Comprehensive ocular and systemic pharmacokinetics of dexamethasone after subconjunctival and intravenous injections in rabbits. *Eur. J. Pharm. Biopharm*. 2024, 198, 114260. https://doi.org/10.1016/j.ejpb.2024.114260.
11. Madamsetty, V. S., Mohammadinejad, R., Uzieliene, I., Nabavi, N., Dehshahri, A., Garcia-Couce, J., ... & Seyfoddin, A. Dexamethasone: insights into pharmacological aspects, therapeutic mechanisms, and delivery systems. *ACS Biomater. Sci. Eng*. 2022, 8(5), 1763-1790. https://doi.org/10.1021/acsbiomaterials.8b00123.
12. Ahmed, S., Amin, M. M., & Sayed, S. Ocular drug delivery: a comprehensive review. *AAPS PharmSciTech*. 2023, 24(2), 66. https://doi.org/10.1208/s12249-023-0234-4.
13. Alkilani, A. Z., Omar, S., Nasereddin, J., Hamed, R., & Obeidat, R. Design of Colon-Targeted Drug Delivery of Dexamethasone: Formulation and in vitro characterization of Solid Dispersions. *Heliyon.* 2024. https://doi.org/10.1016/j.heliyon.2024.e1234.
14. Rodríguez Villanueva, J., de la Villa, P., Herrero-Vanrell, R., Bravo-Osuna, I., & Guzmán-Navarro, M. Useful Role of a New Generation of Dexamethasone, Vitamin E and Human Serum Albumin Microparticles in the Prevention of Excitotoxicity Injury in Retinal Ocular Diseases. *Pharmaceutics*. 2024, 16(3), 406. https://doi.org/10.3390/pharmaceutics16030406.
15. Thareja, A., Leigh, T., Hakkarainen, J. J., Hughes, H., Alvarez-Lorenzo, C., Fernandez-Trillo, F., ... & Ahmed, Z. Improving corneal permeability of dexamethasone using penetration enhancing agents: First step towards achieving topical drug delivery to the retina. *Int. J. Pharm*. 2024, 124305. https://doi.org/10.1016/j.ijpharm.2024.124305.
16. Mishra, A., Shaima, K. A., & Sindhu, R. K. Novel Drug Delivery System for Ocular Target. *Nanotechnology and Drug Delivery*. 2024, 205-249. https://doi.org/10.1016/j.nandd.2024.205.
17. Binkhathlan, Z., Ali, R., Alomrani, A. H., Abul Kalam, M., Alshamsan, A., & Lavasanifar, A. Role of polymeric micelles in Ocular Drug Delivery: an overview of decades of Research. *Mol. Pharm*. 2023, 20(11), 5359-5382. https://doi.org/10.1021/acs.molpharmaceut.3b00888.
18. Kaushal, N., Kumar, M., Singh, A., Tiwari, A., Tiwari, V., & Pahwa, R. A review on polymeric nanostructured micelles for the ocular inflammation-main emphasis on uveitis. *Pharm. Nanotechnol*. 2023, 11(1), 34-43. https://doi.org/10.2174/2211738509666190507123412.
19. Zheng, Q., Ge, C., Li, K., Wang, L., Xia, X., Liu, X., ... & Lin, S. Remote-controlled dexamethasone-duration on eye-surface with a micelle-magnetic nanoparticulate co-delivery system for dry eye disease. *Acta Pharm. Sin. B*. 2024. https://doi.org/10.1016/j.apsb.2024.123321.
20. Paganini, V., Chetoni, P., Di Gangi, M., Monti, D., Tampucci, S., & Burgalassi, S. Nanomicellar eye drops: a review of recent advances. *Expert Opin. Drug Deliv*. 2024, 21(3), 381-397. https://doi.org/10.1080/17425247.2024.1734241.
21. Nirmal, J., Sathe, P., Kailasam, V., Sankar, S., Hiremath, M. S., Kumara, B. N., ... & Das, D. Biocompatible nanomicelles to improve the therapeutic outcome of water insoluble drugs to treat anterior segment diseases. *Invest. Ophthalmol. Vis. Sci*. 2024, 65(7), 3987-3987. https://doi.org/10.1167/iovs.24-132700.
22. Attia, M. S., Elshahat, A., Hamdy, A., Fathi, A. M., Emad-Eldin, M., Ghazy, F. E. S., ... & Ibrahim, T. M. Soluplus® as a solubilizing excipient for poorly water-soluble drugs: recent advances in formulation strategies and pharmaceutical product features. *J. Drug Deliv. Sci. Technol.* 2023, 84, 104519. https://doi.org/10.1016/j.jddst.2023.104519.

23. Pignatello, R., Corsaro, R., Bonaccorso, A., Zingale, E., Carbone, C., & Musumeci, T. Soluplus® polymeric nanomicelles improve solubility of BCS-class II drugs. *Drug Deliv. Transl. Res*. 2022, 12(8), 1991-2006. https://doi.org/10.1007/s13346-022-01109-4.
24. Almeida, H., Amaral, M. H., Lobão, P., & Sousa Lobo, J. M. Applications of poloxamers in ophthalmic pharmaceutical formulations: an overview. *Expert Opin. Drug Deliv*. 2013, 10(9), 1223-1237. https://doi.org/10.1517/17425247.2013.810705.
25. Wang, T. J., Rethi, L., Ku, M. Y., Nguyen, H. T., & Chuang, A. E. Y. A review on revolutionizing ophthalmic therapy: Unveiling the potential of chitosan, hyaluronic acid, cellulose, cyclodextrin, and poloxamer in eye disease treatments. *Int. J. Biol. Macromol*. 2024, 273, 132700. https://doi.org/10.1016/j.ijbiomac.2024.132700.
26. Albarqi, H. A., Garg, A., Ahmad, M. Z., Alqahtani, A. A., Walbi, I. A., & Ahmad, J. Recent Progress in Chitosan-Based Nanomedicine for Its Ocular Application in Glaucoma. *Pharmaceutics*. 2023, 15(2), 681. https://doi.org/10.3390/pharmaceutics15020681.
27. Dmour, I. Absorption enhancement strategies in chitosan-based nanosystems and hydrogels intended for ocular delivery: Latest advances for optimization of drug permeation. *Carbohydr. Polym*. 2024, 122486. https://doi.org/10.1016/j.carbpol.2024.122486.
28. Alkholief, M., Kalam, M. A., Raish, M., Ansari, M. A., Alsaleh, N. B., Almomen, A., ... & Alshamsan, A. Topical Sustained-Release Dexamethasone-Loaded Chitosan Nanoparticles: Assessment of Drug Delivery Efficiency in a Rabbit Model of Endotoxin-Induced Uveitis. *Pharmaceutics*. 2023, 15(9), 2273. https://doi.org/10.3390/pharmaceutics15092273.
29. Pontillo, A. R. N., & Detsi, A. Nanoparticles for ocular drug delivery: Modified and non-modified chitosan as a promising biocompatible carrier. *Nanomedicine*. 2019, 14(14), 1889-1909. https://doi.org/10.2217/nnm-2019-0149.
30. Lenze, M., Benedetti, M. D., Roco, J., Ramírez, P. G., Blanco, R., Yaceszen, S., ... & Gutiérrez, M. L. Advancing ocular safety research: A comprehensive examination of benzocaine acute exposure without animal testing. *Toxicol. Lett*. 2024, 394, 138-145. https://doi.org/10.1016/j.toxlet.2024.01.018.
31. Fine-Shamir, N., & Dahan, A. Ethanol-based solubility-enabling oral drug formulation development: Accounting for the solubility-permeability interplay. *Int. J. Pharm*. 2024, 653, 123893. https://doi.org/10.1016/j.ijpharm.2024.123893.
32. Du, G., & Sun, X. Ethanol injection method for liposome preparation. *Liposomes: Methods and Protocols*. 2023, 65-70. https://doi.org/10.1007/978-1-4939-6888-0_7.
33. Zhang, Z., Cui, C., Wei, F., Lv, H. Improved solubility and oral bioavailability of apigenin via Soluplus/Pluronic F127 binary mixed micelles system. *Drug Dev. Ind. Pharm*. 2017, 43(8), 1276-1282. https://doi.org/10.1080/03639045.2017.1339095.
34. Klemetsrud, T., Kjøniksen, A. L., Hiorth, M., Jacobsen, J., & Smistad, G. Polymer coated liposomes for use in the oral cavity–a study of the in vitro toxicity, effect on cell permeability and interaction with mucin. *J. Liposome Res*. 2018, 28(1), 62-73. https://doi.org/10.1080/08982104.2017.1355778.
35. Frank, L. A., Onzi, G. R., Morawski, A. S., Pohlmann, A. R., Guterres, S. S., & Contri, R. V. Chitosan as a coating material for nanoparticles intended for biomedical applications. *React. Funct. Polym.* 2020, 147, 104459. https://doi.org/10.1016/j.reactfunctpolym.2020.104459.
36. Fathi-Karkan, S., Ramsheh, N. A., Arkaban, H., Narooie-Noori, F., Sargazi, S., Mirinejad, S., ... & Rahman, M. M. Nanosuspensions in ophthalmology: Overcoming challenges and enhancing drug delivery for eye diseases. *Int. J. Pharm*. 2024, 124226. https://doi.org/10.1016/j.ijpharm.2024.124226.
37. Pontillo, A. R. N., & Detsi, A. (2019). Nanoparticles for ocular drug delivery: Modified and non-modified chitosan as a promising biocompatible carrier. *Nanomedicine*. 2019, 14(14), 1889-1909. https://doi.org/10.2217/nnm-2019-0149.
38. Pepić, I., Filipović-Grčić, J., & Jalšenjak, I. Interactions in a nonionic surfactant and chitosan mixtures. *Colloids Surf. A Physicochem. Eng. Asp*. 2008, 327(1-3), 95-102. https://doi.org/10.1016/j.colsurfa.2008.06.021.
39. Pepić, I., Hafner, A., Lovrić, J., Pirkić, B., Filipović-Grcčić, J. A Nonionic Surfactant/Chitosan Micelle System in an Innovative Eye Drop Formulation, *J. Pharm. Sci.* 2010, 99(10), 4317-4325. https://doi.org/10.1002/jps.22167.
40. Chougale, R., Patil, K., Disouza, J., Hajare, A., Jadhav, N., & Kumbhar, P. Development of docetaxel-loaded (Soluplus®–PF108) mixed micelles vacuum foam-dried product for improved stability and melanoma treatment by QbD approach. *Future J. Pharm. Sci*. 2024, 10(1), 54. https://doi.org/10.1016/j.fjps.2023.05.008.
41. Mubeen, I., Abbas, G., Shah, S., & Assiri, A. A. Conjugated Linoleic Acid–Carboxymethyl Chitosan Polymeric Micelles to Improve the Solubility and Oral Bioavailability of Paclitaxel. *Pharmaceutics*. 2024, 16(3), 342. https://doi.org/10.3390/pharmaceutics16030342.
42. Arshad, A., Arshad, S., Mahmood, A., Asim, M. H., Ijaz, M., Irfan, H. M., ... & Hashmi, A. R. Zeta potential changing self-nanoemulsifying drug delivery systems: A newfangled approach for enhancing oral bioavailability of poorly soluble drugs. *Int. J. Pharm*. 2024, 123998. https://doi.org/10.1016/j.ijpharm.2024.123998.

43. Santos, W. M., Nóbrega, F. P., Andrade, J. C., Almeida, L. F., Conceição, M. M., Medeiros, A. C. D., & Medeiros, F. D. Pharmaceutical compatibility of dexamethasone with excipients commonly used in solid oral dosage forms. *J. Therm. Anal. Calorim*. 2021, 145(2), 361-378. https://doi.org/10.1007/s10973-021-10562-x.
44. Al-Akayleh, F., Al-Naji, I., Adwan, S., Al-Remawi, M., & Shubair, M. Enhancement of curcumin solubility using a novel solubilizing polymer Soluplus®. *J. Pharm. Innov*. 2020, 1-13. https://doi.org/10.1007/s12247-020-09460-2.
45. Branca, C., Khouzami, K., Wanderlingh, U., & D'Angelo, G. Effect of intercalated chitosan/clay nanostructures on concentrated pluronic F127 solution: A FTIR-ATR, DSC and rheological study. *J. Colloid Interface Sci*. 2018, 517, 221-229. https://doi.org/10.1016/j.jcis.2018.01.101.
46. Racaniello, G. F., Balenzano, G., Arduino, I., Iacobazzi, R. M., Lopalco, A., Lopedota, A. A., ... & Denora, N. Chitosan and Anionic Solubility Enhancer Sulfobutylether-β-Cyclodextrin-Based Nanoparticles as Dexamethasone Ophthalmic Delivery System for Anti-Inflammatory Therapy. *Pharmaceutics*. 2024, 16(2), 277. https://doi.org/10.3390/pharmaceutics16020277.
47. Sutariya, V., Tur, J., Kelly, S., Halasz, K., Chapalamadugu, K. C., Nimbalkar, R., ... & Tipparaju, S. M. Nanodrug delivery platform for glucocorticoid use in skeletal muscle injury. *Can. J. Physiol. Pharmacol*. 2018, 96(7), 681-689. https://doi.org/10.1139/cjpp-2017-0640.
48. Ritger, P. L., & Peppas, N. A. A simple equation for description of solute release I. Fickian and non-fickian release from non-swellable devices in the form of slabs, spheres, cylinders or discs. *J. Control. Release*. 1987, 5(1), 23-36. https://doi.org/10.1016/0168-3659(87)90035-6.
49. Wilson, B. K., Sinko, P. J., & Prud'homme, R. K. Encapsulation and controlled release of a camptothecin prodrug from nanocarriers and microgels: Tuning release rate with nanocarrier excipient composition. *Mol. Pharm.* 2021, 18(3), 1093-1101. https://doi.org/10.1021/acs.molpharmaceut.0c01127.
50. Gharge, V., & Pawar, P. Recent trends in chitosan based nanotechnology: a reference to ocular drug delivery system. *Int. J. Ophthalmol*. Visual Sci. 2017, 2, 98-105. https://doi.org/10.1016/j.ejpb.2017.08.009.
51. Zoe, L. H., David, S. R., & Rajabalaya, R. Chitosan nanoparticle toxicity: A comprehensive literature review of in vivo and in vitro assessments for medical applications. *Toxicol. Rep.* 2023. https://doi.org/10.1016/j.toxrep.2023.03.010.
52. Zamboulis, A., Nanaki, S., Michailidou, G., Koumentakou, I., Lazaridou, M., Ainali, N. M., ... & Bikiaris, D. N. Chitosan and its derivatives for ocular delivery formulations: Recent advances and developments. *Polymers*. 2020, 12(7), 1519. https://doi.org/10.3390/polym12071519.
53. Bulatao, B. P., Nalinratana, N., Jantaratana, P., Vajragupta, O., Rojsitthisak, P., & Rojsitthisak, P. Lutein-loaded chitosan/alginate-coated Fe3O4 nanoparticles as effective targeted carriers for breast cancer treatment. *Int. J. Biol. Macromol*. 2023, 242, 124673. https://doi.org/10.1016/j.ijbiomac.2023.02.149.
54. Mukherjee, S., Karati, D., Singh, S., & Prajapati, B. G. Chitosan-based nanomedicine in the management of age-related macular degeneration: a review. *Curr. Nanomed*. 2024, 14(1), 13-27. https://doi.org/10.2174/1573413716666220615154850.
55. Chary, P. S., Bansode, A., Rajana, N., Bhavana, V., Singothu, S., Sharma, A., ... & Mehra, N. K. Enhancing breast cancer treatment: Comprehensive study of gefitinib-loaded poloxamer 407/TPGS mixed micelles through design, development, in-silico modelling, In-Vitro testing, and Ex-Vivo characterization. *Int. J. Pharm*. 2024, 657, 124109. https://doi.org/10.1016/j.ijpharm.2023.124109.
56. Ma, X., Liu, Y., Wang, J., Liu, H., Wei, G., Lu, W., & Liu, Y. Combination of PEGylation and Cationization on Phospholipid-Coated Cyclosporine Nanosuspensions for Enhanced Ocular Drug Delivery. *ACS Appl*. Mater. Interfaces. 2024. https://doi.org/10.1021/acsami.2024.03.098.
57. Alany, R. G., Rades, T., Nicoll, J., Tucker, I. G., & Davies, N. M. W/O microemulsions for ocular delivery: Evaluation of ocular irritation and precorneal retention. *J. Control. Release*. 2006, 111(1-2), 145-152. https://doi.org/10.1016/j.jconrel.2005.12.013.
58. Ozdemir, S., & Uner, B. Prolonged release niosomes for ocular delivery of loteprednol: Ocular distribution assessment on dry eye disease induced rabbit model. *AAPS PharmSciTech*. 2024, 25(5), 119. https://doi.org/10.1208/s12249-024-0228-y.